Peptides 155 (2022) 170840

Contents lists available at ScienceDirect

Peptides

journal homepage: www.elsevier.com/locate/peptides

MOTS-c promotes muscle differentiation in vitro

Sandra García-Benlloch [a,b], Francisco Revert-Ros [a], Jose Rafael Blesa [a], Rafael Alis [a,c,*]

[a] Facultad de Medicina y Odontología, Universidad Católica de Valencia San Vicente Mártir, c/Quevedo 2, 46001 Valencia, Spain
[b] Escuela de Doctorado, Universidad Católica de Valencia San Vicente Mártir, c/ Quevedo 2, 46001 Valencia, Spain
[c] Present affiliation, Developmental Neurobiology Unit, Instituto de Biomedicina de Valencia IBV-CSIC, Valencia, Spain

ARTICLE INFO

Keywords:
Atrophy
Mitochondria derived peptides
Muscle

ABSTRACT

MOTS-c (mitochondrial open reading frame of the 12 S rRNA-c) is a newly discovered peptide that has been shown to have a protective role in whole-body metabolic homeostasis. This could be a consequence of the effect of MOTS-c on muscle tissue. Here, we investigated the role of MOTS-c in the differentiation of human (LHCN-M2) and murine (C2C12) muscle progenitor cells. Cells were treated with peptides at the onset of differentiation or after myotubes had been formed. We identified *in silico* a putative Src Homology 2 (SH2) binding motif in the YIFY region of the MOTS-c sequence, and created a Y8F mutant MOTS-c peptide to explore the role of this region. In both cellular models, treatment with wild-type MOTS-c peptide increased myotube formation whereas treatment with the Y8F peptide did not. MOTS-c wild-type, but not Y8F peptide, also protected against interleukin-6 (IL-6)-induced reduction of nuclear myogenin staining in myocytes. Thus, we investigated whether MOTS-c interacts with the IL-6/Janus kinase/ Signal transducer and activator of transcription 3 (STAT3) pathway, and found that MOTS-c, but not the Y8F peptide, blocked the transcriptional activity of STAT3 induced by IL-6. Altogether, our findings suggest that, in muscle cells, MOTS-c interacts with STAT3 via the putative SH2 binding motif in the YIFY region to reduce STAT3 transcriptional activity, which enhances myotube formation. This newly discovered mechanism of action highlights MOTS-c as a potential therapeutic target against muscle-wasting in several diseases.

1. Introduction

MOTS-c (mitochondrial open reading frame of the 12 S rRNA-c) is a 16 amino acid peptide encoded in the 12 S ribosomal RNA region of human mitochondrial DNA. The peptide has been detected in human and murine plasma and in multiple murine tissues [20]. The first reported effect of MOTS-c was in regulating insulin sensitivity and metabolic homeostasis through the 5'-adenosine monophosphate-activated protein kinase (AMPK) pathway in a murine model [20]. Through an effect on muscle tissue, MOTS-c has been proposed to play an important role in maintaining metabolic balance and healthy aging [1]. Subsequently, MOTS-c was shown to translocate to the nucleus and regulate gene expression under stress conditions [16]. These findings highlight MOTS-c as a mitochondrion-derived signal that can directly influence nuclear gene expression, which updates the paradigm for mitochondrial–nuclear communication [3].

To date, a number of published studies have implicated MOTS-c in a variety of cellular and physiological processes, including mitochondrial network dynamics [21], autoimmune diabetes [17], thermogenic gene expression [23], metabolic dysfunctions [17,20] or aging [9,25], among others.

The apparent expansive regulatory effects of MOTS-c on metabolism might indicate that the peptide has an important role in skeletal muscle. Indeed, MOTS-c expression in human skeletal muscle is increased as a result of high-intensity exercise, and exogenous treatment with MOTS-c improves aerobic capacity in a murine model [25]. Moreover, MOTS-c is released into the circulation and freely traverses cellular membranes [16]. Therefore, MOTS-c could have an autocrine function regulating the adaptability of skeletal muscle to exercise and other physiological stimuli.

Here, we investigated the effect of MOTS-c on skeletal muscle tissue growth and repair. We used in vitro cellular models of human and murine myoblasts and analyzed the effect of MOTS-c on muscle differentiation and myotube formation. We show that MOTS-c enhances myotube formation and that this effect depends on the presence of tyrosine residue 8 in a putative Src Homology 2 (SH2) binding motif of the peptide. Also, we found that MOTS-c interacts via its putative SH2 motif with the interleukin-6 / Janus Kinase / Signal transducer and

* Correspondence to: Developmental Neurobiology Unit, Instituto de Biomedicina de Valencia IBV-CSIC, C/ Jaume Roig, 11, 46010 Valencia, Spain.
E-mail address: ralis@ibv.csic.es (R. Alis).

https://doi.org/10.1016/j.peptides.2022.170840
Received 9 May 2022; Received in revised form 22 June 2022; Accepted 10 July 2022
Available online 14 July 2022

activator of transcription 3 (IL-6/JAK/STAT3) pathway, down-regulating the transcriptional activity of STAT3 induced by IL-6.

2. Materials & methods

2.1. Cell lines

The LHCN-M2 cell line of immortalized myoblasts was obtained from Evercyte GmbH (CkHT-040-231-2, Austria). This cell line was derived from muscle tissue of a healthy male donor and immortalized by constitutive expression of the telomerase catalytic subunit and cyclin dependent kinase 4 [35]. LHCN-M2 myoblasts were cultured in tissue culture flasks coated with 0.1 % pig gelatin (Sigma-Aldrich, Germany) in basal medium: 4:1 high-glucose DMEM/M199 (Biowest, France), 4 mM L-glutamine (Biowest), 20 mM HEPES (Biowest), 0.03 μg/mL $ZnSO_4$ (Sigma-Aldrich), 1.4 μg/mL vitamin B12 (Sigma-Aldrich), 55 ng/mL dexamethasone (Sigma-Aldrich), 2.5 ng/mL hepatocyte growth factor (Merck-Millipore, MA, USA) 10 ng/mL fibroblast growth factor (PeproTech, NJ, USA) and 15 % fetal bovine serum (FBS, Biowest). LHCN-M2 cultures were allowed to grow until 50–60 % confluence before splitting. LHCN-M2 myoblasts were differentiated by allowing the culture to reach 100 % confluence and switching to differentiation medium: 4:1 high-glucose DMEM/M199 (Biowest), 4 mM L-glutamine (Biowest), 20 mM HEPES (Biowest), 0.03 μg/mL $ZnSO_4$ (Sigma-Aldrich), 1.4 μg/mL vitamin B_{12} (Sigma-Aldrich), 50 μg/mL apo-transferrin (Sigma-Aldrich and 0.5 % FBS (Biowest).

The C2C12 cell line of immortalized murine myoblasts was obtained from the American Type Culture Collection (ATCC, CRL-1772). This cell line was cultivated in tissue flasks in high-glucose DMEM (Biowest), 2 mM L-glutamine (Biowest) and 15 % FBS (Biowest). C2C12 cultures were allowed to grow until 60–70 % confluence before splitting. C2C12 myoblasts were differentiated by reducing the FBS to 1 % when the cultures reached 90–100 % confluence.

The HeLa cell line (cervix adenocarcinoma) was obtained from ATCC (CCL-2). These cells were cultured in tissue flasks in high-glucose DMEM (Biowest), 1 mM pyruvate (Biowest), 2 mM L-glutamine (Biowest) and 10 % FBS (Biowest).

2.2. Peptides and treatments

Three different peptides were designed and obtained from Genscript (the Netherlands): MOTS-c wild-type peptide (WT, MRWQEMGYIFYPRKLR), a peptide substituting tyrosine-8 for a phenylalanine residue (Y8F, MRWQEMGFIFYPRKLR) and a scrambled MOTS-c peptide (MQGLYKRWMYREPFIR). The purities of the purchased peptides were higher than 96.0 %, and the peptides were fully soluble in water. Pilot experiments showed that 10 μM peptide concentration saturate the effects on the recorded variables, thus the peptide concentration used in the culture medium was 10 μM for all experiments. Water was used for the vehicle control. The scrambled peptide was designed using the protein shuffle tool in Gene Infinity (http://www.geneinfinity.org/) and screened for lack of homology to known peptides/proteins using BLAST [2]. Where indicated, cells were also treated with 25 ng/mL interleukin 6 (IL-6, Gibco, MA, USA) from a 0.5 mg/mL stock in 100 mM acetic acid. In the control condition, the same amount of solvent was added.

2.3. Immunofluorescence

For the immunofluorescence experiments, LHCN-M2 and C2C12 cells were seeded and differentiated in 35 mm polymer chambers treated for tissue culture (81156, Ibidi, Germany). Cells were fixed with 4 % formaldehyde (Thermo Scientific, MA, USA) for 15 min at 37º C and permeabilized with 0.2 % Triton X-100 (Sigma-Aldrich) for 15 min in phosphate-buffered saline (PBS). After washing twice with PBS supplemented with 0.05 % Tween-20 (Sigma-Aldrich), the cells were blocked with 1 % bovine serum albumin (BSA, Sigma-Aldrich), 0.1 % Tween-20 in PBS. Then the cells were incubated overnight at 4º C with mouse monoclonal primary antibodies at 1000 ng/mL to stain all heavy-chain myosin isoforms (clone MF-20, 14–6503–82, Themo Scientific) and to stain myogenin transcription factor (clone F5D, 14–5643–82, Thermo Scientific). After washing, secondary antibody (Alexa Fluor 568, A-11004, Thermo Scientific) was added for 1 h at 500 ng/mL at room temperature in the dark. Nuclei were stained with DAPI (4',6-diamidino-2-phenylindole, Thermo Scientific). Images were acquired with a BX41 fluorescence microscope (Olympus, Japan) coupled to a digital camera (DP74, Olympus) using a 10 × (differentiation experiments, 5 fields acquired per chamber) or a 40 × (myogenin expression, 10 fields acquired per chamber) objective lens.

2.4. Image analysis and myogenic index calculations

The immunofluorescence images were analyzed using ImageJ software [26]. In the differentiation experiments, we recorded the total number of nuclei per field and the number of nuclei in each MF-20 positive cell as well as its area. We considered a myotube as a MF-20-positive cell with at least two nuclei in its cytosol. For the myogenin expression experiments, we recorded the number of myogenin-positive nuclei and the total number of nuclei, per field.

We calculated the myogenic index (MI) as follows:

$$MI_n = 100 \times \frac{\sum_{i=n}^{\infty} \text{nuclei in MF} - 20^{+} \text{ cells with } \mathbf{i} \text{ nuclei}}{\sum \textit{All nuclei}}$$

Each MI was calculated by field or accumulating all the observations in each condition across technical replicates.

2.5. Western blot

Protein lysates from murine myotube and HeLa cultures were obtained with RIPA buffer (Thermo Scientific) and were separated electrophoretically in denaturant polyacrylamide 4–12 % gradient gels (Thermo Scientific). Then samples were blotted to a 0.45 μm polyvinylidene difluoride membrane (Thermo Scientific). Blocking was achieved with 5 % BSA in Tris-buffered saline containing 0.05 % Tween-20 (Thermo Scientific). After washing, blots were incubated overnight with agitation at 4º C with primary antibodies against: STAT3 (clone 124H6, 9139, Cell Signaling Technologies, CST, MA, USA, dilution: 1:1000), phospho-STAT3 Tyr705 (clone D3A7, 9145, CST, dilution: 1:1000) and alpha tubulin (clone TU-02, sc-8035, Santa Cruz Biotechnology, CA, USA, concentration: 500 ng/mL). Then, blots were incubated with suitable horseradish peroxidase (HRP)-labeled secondary antibodies (40 ng/mL). Membranes were visualized by chemiluminescence detection (Las4000, GE Health Care, IL, USA) and band intensity was measured using ImageJ software [26].

2.6. Luciferase assays

We constructed a STAT3 luciferase reporter vector by cloning in a pGL4.11 plasmid (Promega, WI, USA) four sis-inducible element (SIE, 5'-TTCCCGTAAA-3') sites that are actioned by STAT3 in response to IL-6 treatment [32], along with a minimal promoter sequence upstream of the luciferase ORF. The pGL4.11 plasmid was digested with *KpnI/HindIII* and ligated with the 5'-phosphorylated hybridized oligonucleotides listed in Table S1.

HeLa cells were seeded in 6-wells plates and transfected (Fugene HD, Promega) the next day with the STAT3 luciferase reporter. After an additional 24 h, the transfected cells were reseeded in 24-well plates and further cultured for 24 h. Subsequently, the cells were treated with peptides (10 μM) and/or IL-6 (25 ng/mL) for 3 h. Then, the cells were washed with PBS, and luciferase assays were performed in triplicate using the Rapid Detection Firefly Luciferase Activity assay system (Promega) following the manufacturer's instructions with a plate reader

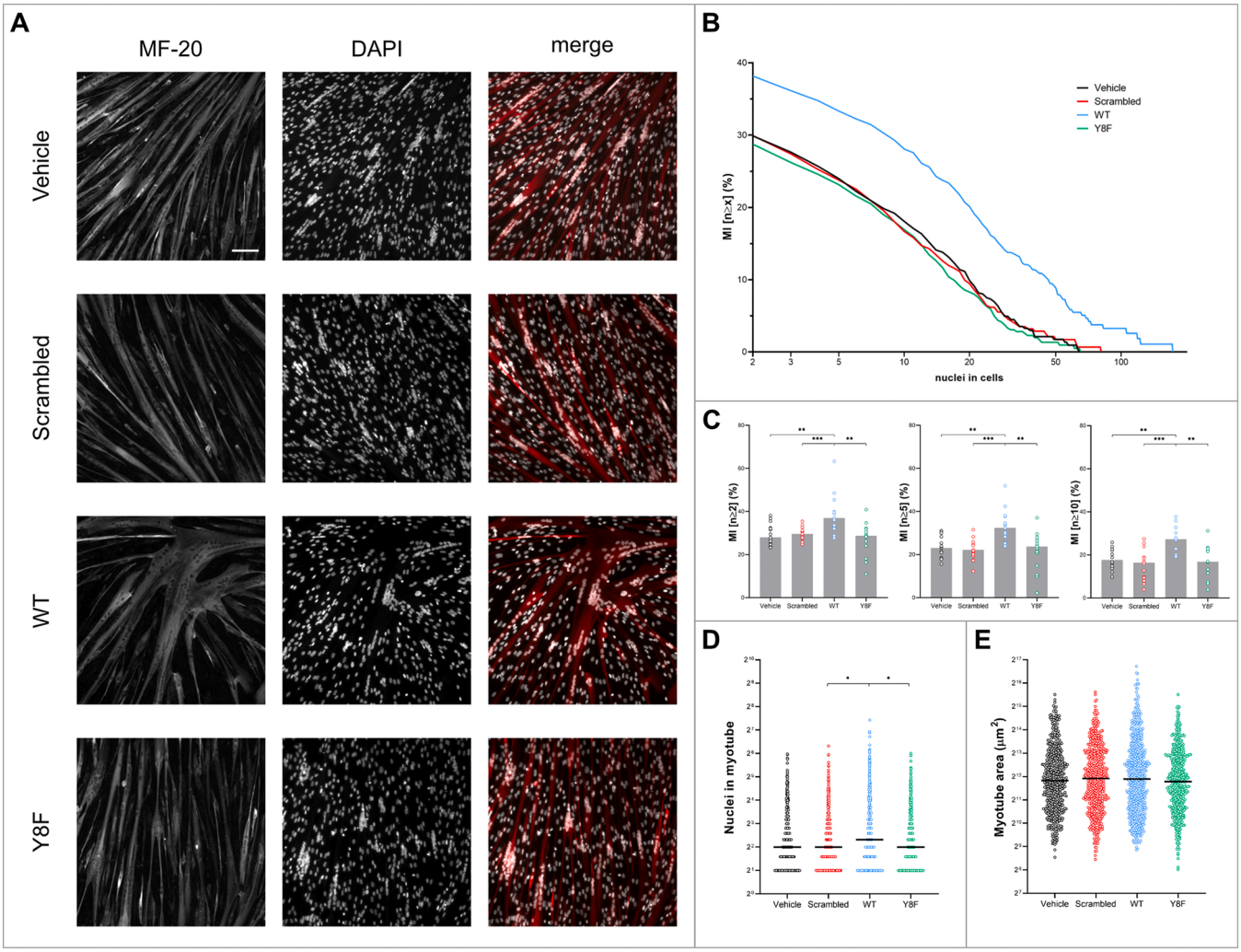

Fig. 1. Effects of MOTS-c treatment on human myotube formation. LHCN-M2 human myoblasts were differentiated for 4 days in the presence of 10 μM peptides (scrambled, WT, Y8F) or vehicle. A) Representative immunofluorescence images of cell cultures stained with MF-20 antibody to visualize myosin heavy chain as a differentiation marker and DAPI to visualize nuclei. B) Myogenic index (MI) representing the number of myotubes containing n = 2 to > 100 nuclei per myotube (all replicates accumulated). C) MI for myotubes with at least 2, 5 or 10 nuclei (per field). D) Nuclei number per myotube. E) Myotube area. Data from three independent experiments (vehicle: 545 myotubes, 13,403 nuclei; scrambled: 504 myotubes, 11,868 nuclei; WT: 590 myotubes, 15,925 nuclei; Y8F: 530 myotubes, 13,044 nuclei). Scale bar = 100 μm. Bars and horizontal lines show median values, symbols represent all replicates. * $p < .05$, ** $p < .01$, *** $p < .001$ in *post-hoc* comparisons using the Kruskal-Wallis test.

(Victor X5, PerkinElmer, MA, USA).

2.7. Statistical analysis

The normality of the distributions of continuous variables was analyzed by using the Kolmogorov-Smirnov test. Since all variables showed non-normal distributions, data were expressed as medians [25th-75th percentiles]. The effect of peptide treatments was analyzed by using the Kruskal-Wallis test. Post hoc comparisons were made with Dunn's correction. The effect of IL-6 treatment was assessed by applying the Mann-Whitney test. The statistical analysis was performed using GraphPad Prism 8.0.2 for Windows (GraphPad, CA, USA).

3. Results

3.1. MOTS-c contains a possible SH2 binding motif

Previously published reports have shown that alterations of the MOTS-c amino acid sequence can modify the biological properties of the peptide [9,33]. In particular, the internal YIFY region (amino acids 8–11) is necessary for MOTS-c to translocate to the nucleus [16]. We used the eukaryotic linear motif (ELM) prediction tool (http://elm.eu.org/) [19] to further explore the presence of functional motifs in the amino acid sequence of MOTS-c. We found a significant probability that the YIFY motif could constitute an SH2 binding motif ($p = .003$). Proteins that contain SH2 domains often participate in the transduction of cellular signals [22]. To be recognized, SH2 binding motifs need to be phosphorylated on a tyrosine residue [14]. Therefore, to further explore the functionality of the YIFY motif, we tested *in silico* whether tyrosine-8 (Y8) or tyrosine-11 (Y11) of MOTS-c could be phosphorylated, by using the NetPhos 3.1 (https://services.healthtech.dtu.dk/service.php?NetPhos-3.1) [4] and KinasePhos 2.0 (https://bio.tools/kinasephos_2.0) [31] bioinformatic tools. Both programs yielded a significant probability for Y8 to be phosphorylated in vivo. These results suggested that the YIFY motif may constitute a functional SH2 binding motif. We considered this information when designing subsequent experiments to establish whether the YIFY region plays a role in the biological effects induced by MOTS-c.

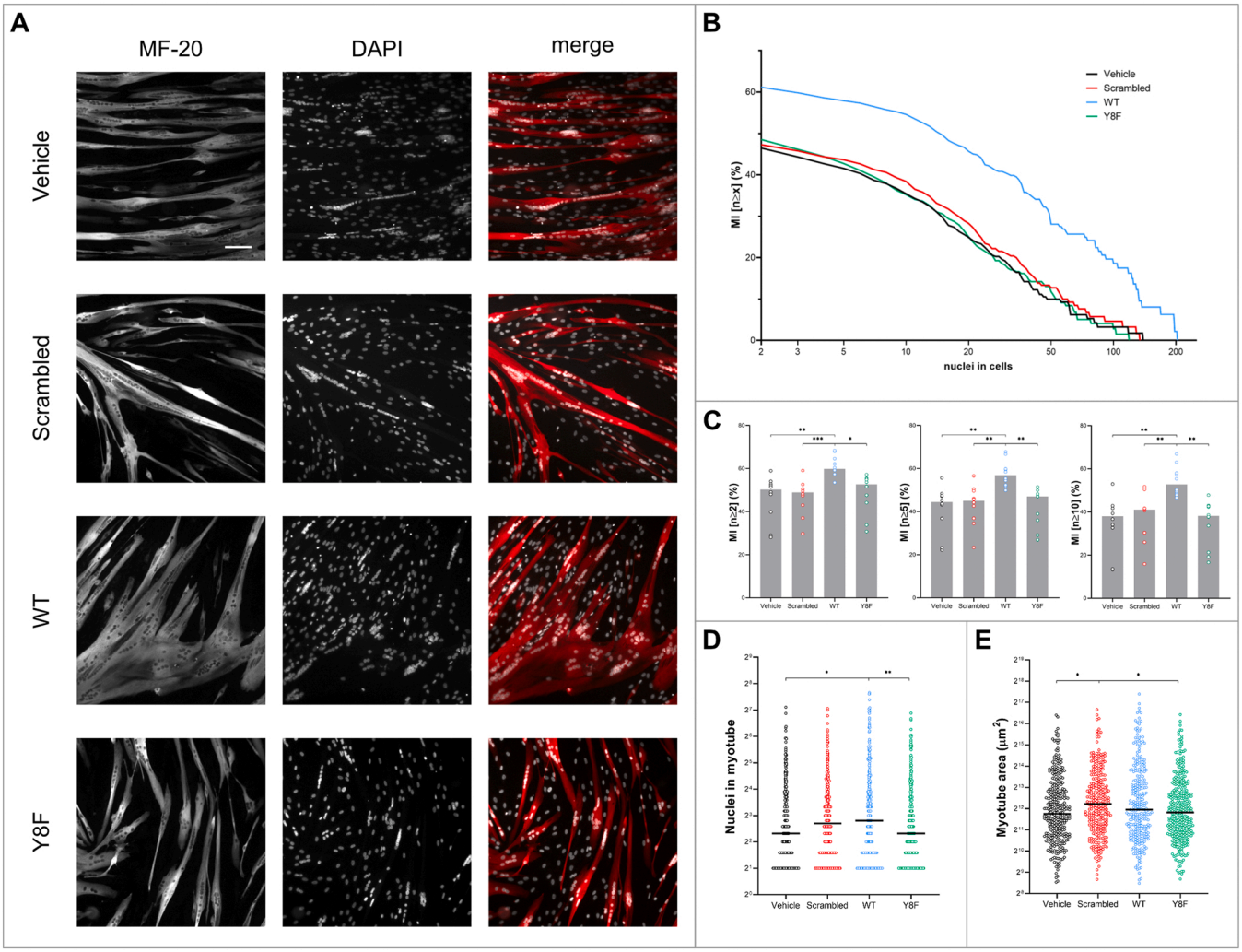

Fig. 2. Effects of MOTS-c treatment on late human myotube formation. LHCN-M2 human myoblasts were differentiated for 4 days and then treated with 10 μM peptides (scrambled, WT, Y8F) or vehicle for an additional 48 h. A) Representative immunofluorescence images of cell cultures stained with MF-20 antibody to visualize myosin heavy chain as a differentiation marker and DAPI to visualize nuclei. B) Myogenic index (MI) representing the number of myotubes containing n = 2 to > 100 nuclei per myotube (all replicates accumulated). C) MI for myotubes with at least 2, 5 or 10 nuclei (per field). D) Nuclei number per myotube. E) Myotube area. Data from two independent experiments (vehicle: 334 myotubes, 7925 nuclei; scrambled: 292 myotubes, 8020 nuclei; WT: 301 myotubes, 9438 nuclei; Y8F: 365 myotubes, 7812 nuclei). Scale bar = 100 μm. Bars and horizontal lines show median values, symbols represent all replicates. * $p < .05$, ** $p < .01$, *** $p < .001$ in *post-hoc* comparisons using the Kruskal-Wallis test.

3.2. MOTS-c treatment increases myotube formation

Several reports have shown that MOTS-c can regulate cellular metabolism, but little is known about the effect of MOTS-c on muscle tissue growth/regeneration. Thus, we examined whether the in vitro differentiation of muscle progenitor cells is affected by MOTS-c. We differentiated both human and murine myoblasts for 4 days in the presence of: wild-type MOTS-c peptide (WT); mutant peptide, in which Y8 was replaced by phenylalanine (Y8F); and, as controls, a peptide containing a scrambled sequence of MOTS-c amino acids, and a vehicle treatment. After 4 days, myosin heavy chain proteins as well as nuclei were detected by immunofluorescence (Fig. 1A). Then the myogenic indexes (MIs) were calculated and represented for all the nuclei amounts found in myotubes (Fig. 1B). The MIs were higher in WT-treated cultures in comparison to control cultures, for both human (Fig. 1B,C) and murine myotubes (Fig. S1B,C). In contrast, the Y8F peptide did not show a myogenic effect. Along the same line, the number of nuclei per myotube was higher in WT-treated (human: 5.0[2.0–11.0], murine: 6.0 [3.0–13.0]) than in scrambled-treated (human: 4.0[2.0–8.0], $p = .022$; murine: 4.0[2.0–9.0], $p < .001$) or Y8F-treated cultures (human: 4.0 [2.0–9.0], $p = .044$; murine: 4.0[2.0–9.0], $p < .001$) (Fig. 1D). Despite the myogenic effect of the WT peptide, we found no differences in myotube area among the four treatment groups in both human (Fig. 1E) and murine cells (Fig. S1E).

Next, we checked whether the myogenic effect of MOTS-c in vitro could also be observed at a late differentiation stage. Thus, myoblast cultures that had been differentiated for 4 (human) or 3 (murine) days were treated with peptides for a further 48 h. As in the previous experiment, the WT peptide increased the MIs in both species whereas the Y8F peptide had no effect (Fig. 2 and Fig. S2). Similarly, the number of nuclei per myotube was higher in the WT-treated cultures (Fig. 2D and Fig. S2D).

3.3. MOTS-c enhances early myogenin expression and protects against IL-6 effects

Expression of the myogenin transcription factor at the onset of differentiation triggers the formation of myotubes [30]. Thus, myogenin is paramount for driving muscle differentiation. We aimed to explore whether MOTS-c treatment influenced myogenin expression after 24 h

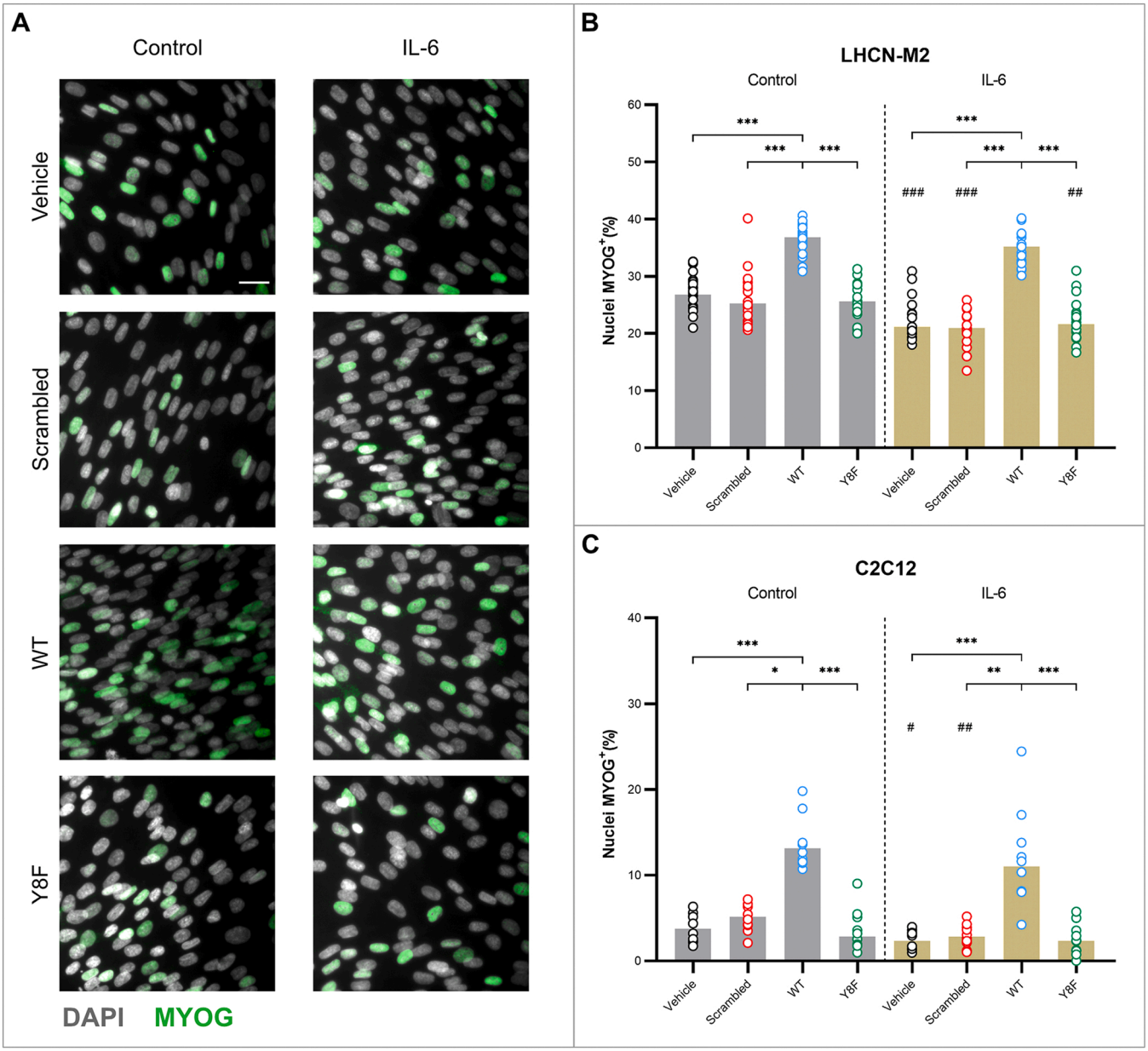

Fig. 3. Effects of MOTS-c and IL-6 on myogenin expression at an early differentiation stage. Human (LHCN-M2) and murine (C2C12) myoblasts were differentiated for 24 h in the presence of 10 μM peptides (vehicle, scrambled, WT or Y8F) and/or IL-6 (25 ng/mL). A) Representative immunofluorescence images of human cell cultures stained for myogenin (MYOG) and nuclei (DAPI). Images of murine cells are not shown. B) Proportion of $MYOG^+$ nuclei in human cell cultures. Data from two independent experiments (nuclei per condition, ranging from 1670 to 2690 per condition). C) Proportion of $MYOG^+$ nuclei in murine cell cultures. Data from one independent experiment (nuclei per condition, ranging from 957 to 1498 per condition). Scale bar = 20 μm. Bars show median values, symbols represent all replicates. * $p < .05$, ** $p < .01$, *** $p < .001$ in *post-hoc* comparisons using the Kruskal-Wallis test. $^{\#}$ $p < .05$, $^{\#\#}$ $p < .01$, $^{\#\#\#}$ $p < .001$ using the Mann-Whitney test.

of differentiation. Moreover, the lack of myogenic effect of the Y8F peptide points to a possible interaction of MOTS-c with a partner containing an SH2 binding domain. A suitable candidate could be a component of the IL-6/JAK/STAT3 pathway which, upon activation by IL-6, triggers atrophic mechanisms in muscle cells [12]. Thus, we combined peptide treatments with IL-6 treatment to explore a possible interaction between MOTS-c and the IL-6/JAK/STAT3 pathway in the regulation of myogenin expression during myoblast differentiation. Fig. 3 shows the effects of treatments on the proportion of myogenin-positive nuclei after 24 h of differentiation. The WT peptide increased the level of myogenin expression whereas the Y8F peptide did not, in both human (Fig. 3B) and murine cells (Fig. 3C). Higher levels of myogenin at an early differentiation stage could explain the myogenic effects of MOTS-c observed in our previous experiments. Interestingly, IL-6 treatment reduced significantly the level of myogenin expression in all cultures except those treated with WT peptide (human: $p = .067$; murine: $p = .197$; Fig. 3B,C).

3.4. MOTS-c interaction with the STAT3 pathway

We sought to explore further the interaction of MOTS-c with the IL-6/JAK/STAT3 pathway. First, we checked the effect of MOTS-c on STAT3 phosphorylation on tyrosine-705 ($STAT3\text{-}pTyr^{705}$), which is required for STAT3 homodimerization and subsequent activation [8, 34]. Thus, we differentiated murine myoblasts for 24 h in the presence of peptides and IL-6 and assayed by western blot the levels of $STAT3\text{-}pTyr^{705}$. We found no effect of peptides on STAT3 phosphorylation in C2C12 cells. Moreover, the increase in $STAT3\text{-}pTyr^{705}$ induced

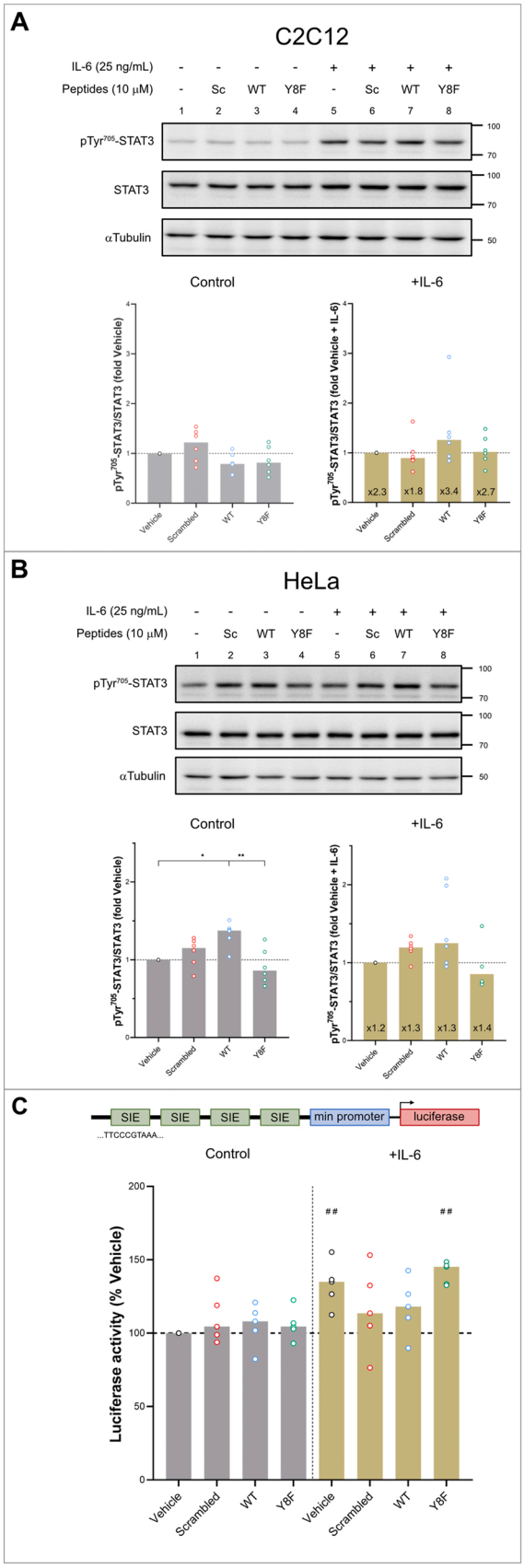

(caption on next column)

Fig. 4. Effects of MOTS-c on STAT3 activation and transcriptional activity. A) C2C12 murine myoblasts were differentiated for 24 h in the presence of 10 μM peptides (vehicle, scrambled, WT or Y8F) and/or IL-6 (25 ng/mL). Activation of STAT3 (phosphorylation on tyrosine 705) was assessed by western blot. Data are expressed as percentage of the vehicle, from 3 independent biological replicates and 6 western blots. B) Activation of STAT3 in HeLa cells incubated for 3 h with 10 μM peptides (vehicle, scrambled, WT or Y8F) and/or IL-6 (25 ng/mL). Data are expressed as percentage of the vehicle, from three independent biological replicates and six western blots. C) HeLa cells were transfected with the STAT3 reporter, reseeded and treated for 3 h with 10 μM peptides (vehicle, scrambled, WT or Y8F) and/or IL-6 (25 ng/mL), then luciferase activity was recorded. Data from five independent biological replicates are shown. Data are expressed as percentage of the vehicle non-IL-6 condition. Bars show median values, symbols represent all replicates. * $p < .05$, ** $p < .01$, *** $p < .001$ in *post-hoc* comparisons using the Kruskal- Wallis test. # $p < .05$, ## $p < .01$, ### $p < .001$ using the Mann-Whitney test.

by IL-6 was similar in all the peptide conditions tested (Fig. 4A).

We switched to the human HeLa cell line that allows higher transfection efficiency to examine whether MOTS-c affects the STAT3 transcriptional activity induced by IL-6. First, we checked the effect of peptide treatments on STAT3 activation. We treated HeLa cells with peptides and IL-6 for 3 h and then quantified STAT3-pTyr^{705} by western blot. We found that STAT3 phosphorylation was slightly increased in the cultures treated with the WT peptide (1.38[1.22–1.43]) in comparison to the vehicle ($p = .043$) or the cells treated with the Y8F peptide (0.86 [0.72–1.14], $p = .007$). However, no effect of peptides was found in the IL-6 treated cells and the effect of IL-6 on STAT3-pTyr^{705} was similar in all conditions (Fig. 4B).

To investigate the transcriptional activity of STAT3, we constructed a STAT3 luciferase reporter containing four SIE sites (5'-TTCCCGTAAA-3') that are bound by STAT3 in response to IL-6 [32]. We transfected the reporter into HeLa cells and, after 24 h, the culture medium was supplemented with the various peptides in combination with IL-6 for 3 h. No significant increase in reporter activity was observed when cells were treated with peptides only (Fig. 4C). However, addition of IL-6 increased the luciferase activity only in the vehicle (135.0[119.8–145.7] %, $p = .008$) and Y8F (136.6[123.8–143.0] %, $p = .008$) conditions (Fig. 4C). Cells treated with WT peptide along with IL-6 did not show an increase in reporter activity ($p = .0310$), which indicates that the transcriptional activity of STAT3 is impaired by MOTS-c. Surprisingly, the scrambled peptide showed results similar to those of the WT peptide, possibly due to off-target effects.

4. Discussion

We aimed to examine the effect of MOTS-c on muscle differentiation in vitro and found that MOTS-c increases myotube formation in both human and murine muscle cells. Commitment, activation and differentiation of skeletal muscle progenitor cells is a well-known process controlled by a cascade of muscle-specific transcription factors [30]. In particular, myogenin expression at the onset of myoblast differentiation is needed for proper myotube formation [11,24]. Therefore, the effect of MOTS-c on myotube formation might be linked to changes in myogenin expression. Our findings support that idea, since we found that MOTS-c increased myogenin expression in both human and murine myoblasts.

We also found that MOTS-c protected against the deleterious effect on myogenin caused by IL-6 supplementation. Elevated levels of inflammatory cytokines, including IL-6, are associated with muscle-wasting conditions [10]. The effect of IL-6 on skeletal muscle is driven by STAT3, which, when activated by JAK proteins, switches on the expression of atrophic proteins like the muscle-specific E3-ubiquitin ligases MAFbx and MuRF1 [12]. Signal transduction in the IL-6/JAK/STAT3 pathway relies on SH2 binding domains and SH2 binding motifs that are recognized upon tyrosine phosphorylation. Thus, a plausible hypothesis might be that MOTS-c interacts with some protein

in the IL-6/JAK/STAT3 pathway via the putative SH2 binding motif (i.e. YIFY motif), thereby reducing pathway activity and thus down-regulating the atrophic processes in muscle. A recently published paper in that the authors showed an interaction between MOTS-c and STAT3 binding to chromatin in murine hypothalamic proopiomelanocortin (POMC) neurons [15], supports this hypothesis. Our results suggest that MOTS-c, via its YIFY motif, decreases the activity of the IL-6/JAK/STAT3 pathway. STAT3 activation was not affected by peptide treatments. Thus, the proposed interaction of MOTS-c with the IL-6/JAK/STAT3 pathway might take place downstream of JAK-induced STAT3 phosphorylation. In fact, MOTS-c decreased the transcriptional activity of STAT3, being the YIFY motif needed for this effect. Upon phosphorylation of its tyrosine residue on the SH2 binding motif, STAT3 homodimerizes and the complex is translocated to the nucleus to exert its transcriptional activity on target genes [8,34]. Our findings might suggest that MOTS-c interferes with STAT3 homodimerization, thus reducing its transcriptional activity. However, this compelling hypothesis should be tested experimentally.

A recent study showed the effects of MOTS-c on myotube formation in C2C12 murine cells. In that report, no significant effect of MOTS-c on the number of myotubes per field or their diameter was found, although no MI data were provided [18]. However, MOTS-c protected against atrophy induced by palmitic acid in C2C12 cells, and its administration to obese mice reduced myostatin expression by activating the mTORC2-AKT-FOXO1 pathway [18]. This mechanism could partly contribute to the myogenic effect of MOTS-c, although, we did not find an effect of MOTS-c activating insulin signaling in our experimental models (data not shown). Nevertheless, the protective effect of MOTS-c against IL-6-induced reduction of myogenin and IL-6-induced STAT3 transcriptional activity prove that MOTS-c interacts with the IL-6/JAK/STAT3 pathway to reduce its impact on myotube formation. Furthermore, the ineffectiveness of the Y8F peptide indicates that the putative SH2 binding motif in MOTS-c is needed for the peptide's function. Nevertheless, it should be noted that we did not assay experimentally the phosphorylation of tyrosine-8 in MOTS-c or whether the YIFY motif binds to the SH2 binding domain in STAT3. Future projects should engage these experiments.

Constitutive activation of STAT3 has been previously described as an oncogenic mechanism since it plays a role in cell survival, proliferation, angiogenesis, metastasis, and cell protection against the body's immune response [6]. Hematopoietic disorders such as myeloma and others are linked with STAT3 over-activation [7]. Moreover, continuous cytokine-mediated STAT3 stimulation has been reported in many cases of solid tumors [27]. STAT3 overexpression or hyperactivation in cancers is commonly associated with poor prognosis. Thus, pharmacological inhibitors of STAT3 are currently in development, several of them aiming to bind the SH2 domain [13]. The properties of MOTS-c we showed here suggest that MOTS-c might be a suitable pharmacological target to counter the neoplastic role of STAT3.

The IL-6/JAK/STAT3 pathway has pleiotropic effects on skeletal muscle. A basal level of STAT3 activity is necessary for skeletal muscle satellite cells to develop properly [28,36]. On the other hand, highly-activated STAT3 in skeletal muscle caused by IL-6 in inflammatory contexts drives increased muscle turnover [5,29]. Our findings indicate that MOTS-c might counter the muscle-wasting effects of STAT3 hyperactivation, as well as the pro inflammatory states linked to aging. Further studies using primary cultures and/or murine models could tackle these issues in the future.

In conclusion, MOTS-c has a myogenic effect on myoblast differentiation. The internal hydrophobic YIFY motif of MOTS-c, a putative SH2 binding motif, is key to its interaction with the IL-6/JAK/STAT3 pathway to reduce the transcriptional activity of STAT3 induced by IL-6. This mechanism of interaction opens a range of therapeutic possibilities for MOTS-c to fight against pathologies linked to muscle wasting.

Acknowledgements

We thank Maria Teresa Martinez and Ovsanna Kepenekyan for their technical assistance and to Dr. Jesus Angel Prieto for his help and support.

Compliance with ethical standards

The authors state no conflict of interest. This research does not involve human participants or animals.

Funding

This project has been funded by the Universidad Católica de Valencia (2019-168-002, 2019-168-004, 2020-168-001, 2020-168-002, 2020-168-004). SGB is a predoctoral fellow and RA a postdoctoral fellow of Universidad Católica de Valencia (2018-168-002).

CRediT authorship contribution statement

Sandra García-Benlloch: Methodology, Formal analysis, Investigation. **Francisco Revert:** Methodology, Writing – review & editing. **Jose Rafael Blesa:** Conceptualization, Methodology, Funding acquisition. **Rafael Alis:** Conceptualization, Methodology, Formal analysis, Investigation, Writing – original draft, Writing – review & editing.

Appendix A. Supporting information

Supplementary data associated with this article can be found in the online version at doi:10.1016/j.peptides.2022.170840.

References

[1] R. Alis, A. Lucia, J.R. Blesa, F. Sanchis-Gomar, The role of mitochondrial derived peptides (mdps) in metabolism, J. Cell. Physiol. 230 (12) (2015) 2903–2904. ⟨https://10.1002/jcp.25023⟩.
[2] S.F. Altschul, W. Gish, W. Miller, E.W. Myers, D.J. Lipman, Basic local alignment search tool, J. Mol. Biol. 215 (3) (1990) 403–410. ⟨https://10.1016/s0022-2836⟩(05)80360-2.
[3] Benayoun B.A., Lee C. (2019) Mots-c: A mitochondrial-encoded regulator of the nucleus. 41(9):e1900046. https://10.1002/bies.201900046.
[4] N. Blom, T. Sicheritz-Pontén, R. Gupta, S. Gammeltoft, S. Brunak, Prediction of post-translational glycosylation and phosphorylation of proteins from the amino acid sequence, Proteomics 4 (6) (2004) 1633–1649. ⟨https://10.1002/pmic.200300771⟩.
[5] A. Bonetto, T. Aydogdu, X. Jin, Z. Zhang, R. Zhan, L. Puzis, L.G. Koniaris, T. A. Zimmers, Jak/stat3 pathway inhibition blocks skeletal muscle wasting downstream of il-6 and in experimental cancer cachexia, Am. J. Physiol. Endocrinol. Metab. 303 (3) (2012) E410–E421, https://doi.org/10.1152/ajpendo.00039.2012.
[6] E. Bournazou, J. Bromberg, Targeting the tumor microenvironment: Jak-stat3 signaling, Jak. Stat. 2 (2) (2013), e23828. ⟨https://10.4161/jkst.23828⟩.
[7] R. Crescenzo, F. Abate, E. Lasorsa, F. Tabbo, M. Gaudiano, N. Chiesa, F. Di Giacomo, E. Spaccarotella, L. Barbarossa, E. Ercole, M. Todaro, M. Boi, A. Acquaviva, E. Ficarra, D. Novero, A. Rinaldi, T. Tousseyn, A. Rosenwald, L. Kenner, L. Cerroni, A. Tzankov, M. Ponzoni, M. Paulli, D. Weisenburger, W. C. Chan, J. Iqbal, M.A. Piris, A. Zamo, C. Ciardullo, D. Rossi, G. Gaidano, S. Pileri, E. Tiacci, B. Falini, L.D. Shultz, L. Mevellec, J.E. Vialard, R. Piva, F. Bertoni, R. Rabadan, G. Inghirami, Convergent mutations and kinase fusions lead to oncogenic stat3 activation in anaplastic large cell lymphoma, Cancer Cell 27 (4) (2015) 516–532. ⟨https://10.1016/j.ccell.2015.03.006⟩.
[8] J.E. Darnell Jr., I.M. Kerr, G.R. Stark, Jak-stat pathways and transcriptional activation in response to ifns and other extracellular signaling proteins, Science 264 (5164) (1994) 1415–1421. ⟨https://10.1126/science.8197455⟩.
[9] N. Fuku, H. Pareja-Galeano, H. Zempo, R. Alis, Y. Arai, A. Lucia, N. Hirose, The mitochondrial-derived peptide mots-c: a player in exceptional longevity? Aging Cell 14 (6) (2015) 921–923. ⟨https://10.1111/acel.12389⟩.
[10] F. Haddad, F. Zaldivar, D.M. Cooper, G.R. Adams, Il-6-induced skeletal muscle atrophy, J. Appl. Physiol. 98 (3) (2005) 911–917, https://doi.org/10.1152/japplphysiol.01026.2004.
[11] P. Hasty, A. Bradley, J.H. Morris, D.G. Edmondson, J.M. Venuti, E.N. Olson, W. H. Klein, Muscle deficiency and neonatal death in mice with a targeted mutation in the myogenin gene, Nature 364 (6437) (1993) 501–506. ⟨https://10.1038/364501a0⟩.
[12] Z. Huang, L. Zhong, J. Zhu, H. Xu, W. Ma, L. Zhang, Y. Shen, B.Y. Law, F. Ding, X. Gu, H. Sun, Inhibition of il-6/jak/stat3 pathway rescues denervation-induced

skeletal muscle atrophy, Ann. Transl. Med. 8 (24) (2020) 1681. ⟨https://10.21037/atm-20-7269⟩.
[13] Johnson D.E., O'Keefe R.A., Grandis J.R. (2018) Targeting the il-6/jak/stat3 signalling axis in cancer. 15(4):234–248. https://10.1038/nrclinonc.2018.8.
[14] T. Kaneko, R. Joshi, S.M. Feller, S.S. Li, Phosphotyrosine recognition domains: The typical, the atypical and the versatile, Cell Commun. Signal.: CCS 10 (1) (2012) 32. ⟨https://10.1186/1478-811x-10-32⟩.
[15] G.M. Kang, S.H. Min, C.H. Lee, J.Y. Kim, H.S. Lim, M.J. Choi, S.B. Jung, J.W. Park, S. Kim, C.B. Park, H. Dugu, J.H. Choi, W.H. Jang, S.E. Park, Y.M. Cho, J.G. Kim, K. G. Kim, C.S. Choi, Y.B. Kim, C. Lee, M. Shong, M.S. Kim, Mitohormesis in hypothalamic pomc neurons mediates regular exercise-induced high-turnover metabolism, Cell Metab. 33 (2) (2021) 334–349, e6. ⟨https://10.1016/j.cmet.2021.01.003⟩.
[16] K.H. Kim, J.M. Son, B.A. Benayoun, C. Lee, The mitochondrial-encoded peptide mots-c translocates to the nucleus to regulate nuclear gene expression in response to metabolic stress, Cell Metab. 28 (3) (2018) 516–524, e7. ⟨https://10.1016/j.cmet.2018.06.008⟩.
[17] B.S. Kong, S.H. Min, C. Lee, Y.M. Cho, Mitochondrial-encoded mots-c prevents pancreatic islet destruction in autoimmune diabetes, Cell Rep. 36 (4) (2021), 109447. ⟨https://10.1016/j.celrep.2021.109447⟩.
[18] Kumagai H., Coelho A.R., Wan J., Mehta H.H., Yen K., Huang A., Zempo H., Fuku N., Maeda S., Oliveira P.J., Cohen P., Kim S.-J. (2021) Mots-c reduces myostatin and muscle atrophy signaling. 320(4):E680-E690. https://10.1152/ajpendo.00275.2020.
[19] M. Kumar, M. Gouw, S. Michael, H. Sámano-Sánchez, R. Pancsa, J. Glavina, A. Diakogianni, J.A. Valverde, D. Bukirova, J. Čalyševa, N. Palopoli, N.E. Davey, L. B. Chemes, T.J. Gibson, Elm-the eukaryotic linear motif resource in 2020, Nucleic Acids Res. 48 (D1) (2020) D296–d306, https://doi.org/10.1093/nar/gkz1030.
[20] Lee C., Zeng J., Drew B.G., Sallam T., Martin-Montalvo A., Wan J., Kim S.-J., Mehta H., Hevener A.L., de Cabo R., Cohen P. (2015) The mitochondrial-derived peptide mots-c promotes metabolic homeostasis and reduces obesity and insulin resistance. 21(3):443–454. https://10.1016/j.cmet.2015.02.009.
[21] Q. Li, H. Lu, G. Hu, Z. Ye, D. Zhai, Z. Yan, L. Wang, A. Xiang, Z. Lu, Earlier changes in mice after d-galactose treatment were improved by mitochondria derived small peptide mots-c, Biochem. Biophys. Res. Commun. 513 (2) (2019) 439–445. ⟨https://10.1016/j.bbrc.2019.03.194⟩.
[22] B.A. Liu, E. Shah, K. Jablonowski, A. Stergachis, B. Engelmann, P.D. Nash, The sh2 domain-containing proteins in 21 species establish the provenance and scope of phosphotyrosine signaling in eukaryotes, Sci. Signal. 4 (202) (2011) ra83. ⟨https://10.1126/scisignal.2002105⟩.
[23] H. Lu, S. Tang, C. Xue, Y. Liu, J. Wang, W. Zhang, W. Luo, J. Chen, Mitochondrial-derived peptide mots-c increases adipose thermogenic activation to promote cold adaptation, Int. J. Mol. Sci. 20 (10) (2019). ⟨https://10.3390/ijms20102456⟩.
[24] Y. Nabeshima, K. Hanaoka, M. Hayasaka, E. Esumi, S. Li, I. Nonaka, Y. Nabeshima, Myogenin gene disruption results in perinatal lethality because of severe muscle defect, Nature 364 (6437) (1993) 532–535. ⟨https://10.1038/364532a0⟩.
[25] Reynolds J.C., Lai R.W., Woodhead J.S.T., Joly J.H., Mitchell C.J., Cameron-Smith D., Lu R., Cohen P., Graham N.A., Benayoun B.A., Merry T.L., Lee C. (2021) Mots-c is an exercise-induced mitochondrial-encoded regulator of age-dependent physical decline and muscle homeostasis. 12(1):470. https://10.1038/s41467–020-20790–0.
[26] C.A. Schneider, W.S. Rasband, K.W. Eliceiri, Nih image to imagej: 25 years of image analysis, Nat. Methods 9 (7) (2012) 671–675. ⟨https://10.1038/nmeth.2089⟩.
[27] K.S. Siveen, S. Sikka, R. Surana, X. Dai, J. Zhang, A.P. Kumar, B.K. Tan, G. Sethi, A. Bishayee, Targeting the stat3 signaling pathway in cancer: role of synthetic and natural inhibitors, Biochim. Et. Biophys. Acta 1845 (2) (2014) 136–154. ⟨https://10.1016/j.bbcan.2013.12.005⟩.
[28] M.T. Tierney, T. Aydogdu, D. Sala, B. Malecova, S. Gatto, P.L. Puri, L. Latella, A. Sacco, Stat3 signaling controls satellite cell expansion and skeletal muscle repair, Nat. Med. 20 (10) (2014) 1182–1186. ⟨https://10.1038/nm.3656⟩.
[29] E. Wada, J. Tanihata, A. Iwamura, S. Takeda, Y.K. Hayashi, R. Matsuda, Treatment with the anti-il-6 receptor antibody attenuates muscular dystrophy via promoting skeletal muscle regeneration in dystrophin-/utrophin-deficient mice, Skelet. Muscle 7 (1) (2017) 23. ⟨https://10.1186/s13395-017-0140-z⟩.
[30] Y.X. Wang, M.A. Rudnicki, Satellite cells, the engines of muscle repair, Nat. Rev. Mol. Cell Biol. 13 (2) (2011) 127–133. ⟨https://10.1038/nrm3265⟩.
[31] Y.H. Wong, T.Y. Lee, H.K. Liang, C.M. Huang, T.Y. Wang, Y.H. Yang, C.H. Chu, H. D. Huang, M.T. Ko, J.K. Hwang, Kinasephos 2.0: a web server for identifying protein kinase-specific phosphorylation sites based on sequences and coupling patterns, Nucleic Acids Res. 35 (Web Server issue) (2007) W588–W594. ⟨https://10.1093/nar/gkm322⟩.
[32] E. Yang, L. Lerner, D. Besser, J.E. Darnell Jr., Independent and cooperative activation of chromosomal c-fos promoter by stat3, J. Biol. Chem. 278 (18) (2003) 15794–15799. ⟨https://10.1074/jbc.M213073200⟩.
[33] H. Zempo, S.J. Kim, N. Fuku, Y. Nishida, Y. Higaki, J. Wan, K. Yen, B. Miller, R. Vicinanza, E. Miyamoto-Mikami, H. Kumagai, H. Naito, J. Xiao, H.H. Mehta, C. Lee, M. Hara, Y.M. Patel, V.W. Setiawan, T.M. Moore, A.L. Hevener, Y. Sutoh, A. Shimizu, K. Kojima, K. Kinoshita, Y. Arai, N. Hirose, S. Maeda, K. Tanaka, P. Cohen, A pro-diabetogenic mtdna polymorphism in the mitochondrial-derived peptide, mots-c, Aging 13 (2) (2021) 1692–1717. ⟨https://10.18632/aging.202529⟩.
[34] Z. Zhong, Z. Wen, J.E. Darnell Jr., Stat3: a stat family member activated by tyrosine phosphorylation in response to epidermal growth factor and interleukin-6, Science 264 (5155) (1994) 95–98. ⟨https://10.1126/science.8140422⟩.
[35] C.H. Zhu, V. Mouly, R.N. Cooper, K. Mamchaoui, A. Bigot, J.W. Shay, J.P. Di Santo, G.S. Butler-Browne, W.E. Wright, Cellular senescence in human myoblasts is overcome by human telomerase reverse transcriptase and cyclin-dependent kinase 4: consequences in aging muscle and therapeutic strategies for muscular dystrophies, Aging Cell 6 (4) (2007) 515–523. ⟨https://10.1111/j.1474-9726.2007.00306.x⟩.
[36] H. Zhu, F. Xiao, G. Wang, X. Wei, L. Jiang, Y. Chen, L. Zhu, H. Wang, Y. Diao, H. Wang, N.Y. Ip, T.H. Cheung, Z. Wu, Stat3 regulates self-renewal of adult muscle satellite cells during injury-induced muscle regeneration, Cell Rep. 16 (8) (2016) 2102–2115. ⟨https://10.1016/j.celrep.2016.07.041⟩.